# Interference from Knots, Wave Propagation Direction, and Effect of Juvenile and Reaction Wood on Velocities in Ultrasound Tomography

Stella S. A. Palma, Raquel Gonçalves,* Alex J. Trinca, Cândida Pereira Costa, Mariana N. Reis, and Guilherme A. Martins

Acoustic tomography is based on the velocity variation inside the inspected element. However, wood is heterogeneous and anisotropic, which causes natural velocity variations. In wood, the great challenge to apply this technology is to interpret and differentiate the natural variations of the material from those caused by deterioration. This study aimed to evaluate the interference caused by knots, the wave propagation direction, and the effect of juvenile and reaction wood on the velocities determined *via* ultrasonic tomography. The tests were performed using 40 disks of *Pinus elliottii*. From the results it was concluded that intrinsic orthotropy of the wood was reflected in the wave propagation on the disks with radial velocities greater than the tangential ones, higher velocities in the knot zones, and different velocities in the zones of compression and opposition wood. In the measurements using the diffraction mesh, the edge velocities (tangential direction with the maximum angle from the radial direction) were always lower than all of the other velocities in the disk. More significant variations in the velocity were obtained in the juvenile wood. These results contribute to quantifying some interferences associated with tomography images, such that the misinterpretation can be minimized.

*Keywords: Juvenile wood; Reaction wood; Knots*

*Contact information: Laboratory of Nondestructive Testing – LabEND, School of Agricultural Engineering, FEAGRI University of Campinas - UNICAMP, Brazil;*
** Corresponding author: raquel@feagri.unicamp.br*

## INTRODUCTION

Acoustic tomography in trees analyzes the presence of anomalies or deterioration and is based on the generation of images produced by associating velocity bands with colors. Several types of defects (hollows, cracks, or wood zones deteriorated by fungi and termites) and singularities (knots, resin bags, and reaction wood) can occur in trees. All of these defects and singularities affect the anatomical structure of the material and its local stiffness to various degrees. These variations can be captured by the variations in the wave propagation velocities. However, wood is heterogeneous and anisotropic, which leads to normal variations in velocity that are not the result of any type of decay. Thus, the feasibility is quite low for obtaining reference values from sound wood that can be used as comparative values in acoustic tomography interpretations (Katz *et al*. 2008; Brancheriau *et al.* 2012). One major challenge in acoustic tomography is interpreting the velocity variations in the trunk and differentiating the natural variations of the material from variations caused by decay.

In the wood industry, internal decay in standing trees can cause very high expenditures, particularly in high-priced veneer products (Wang *et al.* 2009). In cities, internal decay cause tree or tree parts to fall and constitute a significant hazard to people and property (Sani *et al*. 2012). Accordingly, numerous studies have focused on the development of analysis tools that allow detection of decay in trees. Acoustic methods can be regarded as very appropriate to achieve this goal. The acoustic tomography for detecting internal decay relating to fungal and termite attack present good accuracy (Gilbert and Smiley 2004), but some parameters, such as internal cracks, can greatly interfere in the accuracy (Wang *et al.* 2009). The influence of wood heterogeneity is also relevant for the accuracy of the technique for the detection of cavities (Schubert *et al.* 2009).

An isolated knot has a different anatomical structure, and it is relatively denser and stiffer than normal wood. Knots cause interruptions in the fibers (hardwoods) and tracheids (conifers) and deviations in the grain, which are mainly responsible for reductions in the strength of the wood. This strength loss as a function of the inclination of the fibers has been well established in the literature (Kollmann and Coté 1984). Recent studies have focused on methods to detect knots and calculate the fiber inclination in the knot region (Guindos and Guaita 2013; Guindos and Polocoser 2015) because this aspect is highly relevant to the wood grade. Many researchers have also studied the effect of knots on wave propagation. It has been found that a decrease in velocity is associated with a decrease in the stiffness, mainly because of the deviation in fibers around knots (Puccini 2002; Bucur 2006). However, these studies focused on the longitudinal direction. When constructing tomographic images, the direction of propagation is perpendicular to the grain, and thus, the effect of a knot on the propagation velocity differs from those observed in wood sorting studies. Riggio *et al.* (2015) noted that in acoustic tomography a high velocity can be associated with the presence of knots, and that such increases in velocity vary according to the size and number of knots in the inspected section.

Reaction wood is considered a natural defect in trees and occurs in response to growing conditions. Reaction wood is called compression wood in softwoods and tension wood in hardwoods, according to the region where it was formed. This type of wood is not desired in structural applications because it is fragile or in applications involving furniture and frames because it exhibits relatively high shrinkage (Haygreen and Bowyer 1995). Thus, methods to recognize this type of wood are important in the timber industry. Because the anatomical structure of reaction wood is different from that of normal wood, the wave propagation method can be used for its detection (Hamm and Lam 1989; Bucur and Chivers 1991; Beall 2002; Pellerin and Ross 2002; Bucur 2003a, 2003b; Saadat-Nia *et al*. 2011).

Another aspect that has been widely studied and reported on in scientific articles and books is juvenile wood. The anatomical structure of juvenile wood is different from that of mature wood because it has larger microfibril angles, shorter cells, fewer latewood cells, thinner cell walls, and a lower density (Haygreen and Bowyer 1995). Because acoustic methods are affected by the anatomical structure, velocity variations are expected to be captured in ultrasonic tests of this type of material. Indeed, lower velocity values in juvenile wood zones have been highlighted in studies using wave propagation (Brancheriau *et al*. 2012).

This study evaluated the interference caused by knots, the wave propagation direction in the trunk cross-section, and the effect of juvenile and reaction wood on the velocities obtained using ultrasonic tomography.

## EXPERIMENTAL

### Materials

The velocities analyzed in this study were obtained from ultrasonic measurements on *Pinus elliottii* disks using an 8-point diffraction mesh (Fig. 1) to generate tomography images. Because the disks were approximately regular, the 8 points were marked equidistantly from the perimeter. In this measurement process, the emitter transducer was fixed at one point, and the receiving transducer picked up the wave at all other points. This procedure was repeated until the transmitter had passed through all 8 points, which resulted in repeated measurements along the same routes (*e.g.*, the transducer emitter at point 1 and the receiver at point 2 *versus* the transducer emitter at point 2 and the receiver at point 1). The average of the measured velocities was used. Thus, with 8 points, 28 paths were measured on each disk.

The tests were performed with conventional ultrasound equipment (USLab, Agricef, Paulínia, Brazil) and exponential-face 45-kHz frequency transducers.

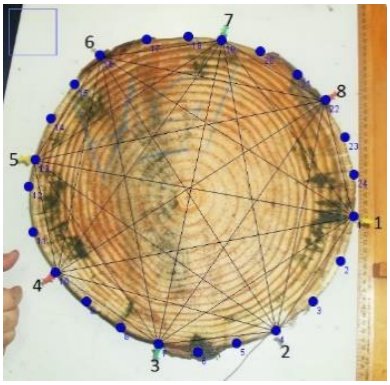


**Fig. 1.** Example of an 8-point diffraction mesh on a *Pinus* sp. disk

For this study, 22 logs were obtained from 11 trees (Itapeva, Brazil) with ages ranging from 6- to 23-years-old, and disks were removed from each log. The disks used in the study were cut as soon as they were removed from the trees and were maintained in saturated conditions until the end of the tests. Because *Pinus* wood is notably susceptible to fungi, a superficial proliferation of staining fungi was observed. However, this did not damage the wood structure, as was confirmed later.

The disks, with approximate140 mm thickness, were evaluated in detail according to the desired specificities, and 40 disks were selected based on the sample composition. The conditions of interest for the composition of the sample were as follows: disks with an approximately centered pith and normal wood, disks with an approximately centered pith and knots, and disks with a displaced pith and compression and opposition wood zones. In the disks with a displaced pith, the areas with compression wood were highlighted. Zones containing reaction wood usually have wider growth rings and dark

wood (Ruelle 2014). Among the disks with displaced piths, six were composed entirely of juvenile wood, which were selected for the tests.

Each disk was photographed next to a scale as a reference to convert the pixel unit to length scale, since the interpolator of the software (ImageWood 3.0) use the scale in centimeters to obtain the tomographic image. This software was developed by this research group (Campinas, Brazil). The use of this software required two spreadsheets: one containing the coordinates of the disk contour and the other containing the coordinates of the measurement points with their respective wave propagation times. To obtain the spreadsheets, ImageJ software (version 1.51p, National Institute of Mental Health, Bethesda, MD, USA) was used. The photographic image file of each disk was opened in this software, and the initial measurement point (point 1) was selected so that the following 7 points were numbered clockwise according to the sequence of the tests.

The routes constituting the diffraction mesh were drawn on each disk (Fig. 1) so that the condition of the wood on different routes and velocity interferences could be analyzed. Therefore, the samples were named according to their conditions as follows: A: disks with an approximately centered pith and normal wood; B: disks with an approximately centered pith and knots; C: disks with a displaced pith and a large volume of mature wood; and D: disks with a displaced pith and juvenile wood.

The disks were numbered according to the log from which they were taken and were individually analyzed. For each route, the numbers were assigned according to Table 1. These numbers were used to statistically analyze the velocities using a multifactor analysis of variance (ANOVA). This analysis considered the variability of different disks to verify the velocity differences in the measurement routes.

**Table 1.** Separation of the Disks in the Samples and Analysis of Each Route According to the Direction and Condition of the Wood

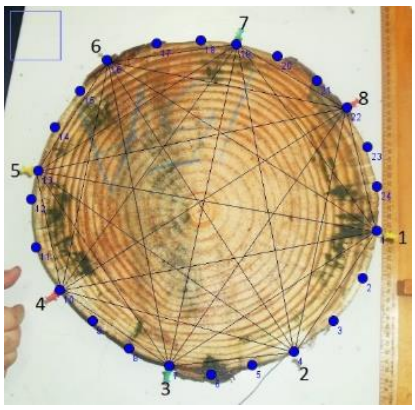


| Number and Type of Route | Sample | | | |
|---|---|---|---|---|
| | A | B | C | D |
| **1**: Tangential edge paths (1-2; 2-3; 3-4; 4-5; 5-6; 6-7; 7-8) | X | X | X | X |
| **2**: Routes that completely pass through the reaction wood zone* | | | X | X |
| **3**: Routes that pass through the opposition wood zone* | | | X | X |
| **4**: All tangential routes | X | X | | |
| **5**: All radial routes | X | X | | |
| **6**: Tangential paths that pass through the knots | | X | | |
| **7**: Radial paths passing through the knots | | X | | |

*Routes that partially pass through zones of compression and opposition wood were not considered;
Legend: A: disks with an approximately centered pith and normal wood; B: disks with an approximately centered pith and knots; C: disks with a displaced pith; and D: juvenile wood disks with a displaced pith

## Methods

The velocities in different measurement routes were statistically analyzed according to the wood condition (Table 1) in different stages. The sample disks in group A were analyzed to verify the difference between the tangential and radial propagation

velocities. In other samples, this analysis could be affected by the wood condition in the wave trajectory (*i.e.*, the presence of knots or reaction wood). The sample disks in group B were used to evaluate the effect of knots on the velocity along the routes that passed through them. Because the pith was approximately centered in these samples, the tangential and radial routes that passed through normal wood without knots were also evaluated. The sample disks in groups C and D were used to evaluate the differences in the velocities in juvenile and mature wood and the effects of reaction wood on the velocity.

For the interference assessment, tomographic images were developed using ImageWood 3.0 software. This software use velocities obtained on routes from diffraction mesh (Figure 1) interpolated using Ellipse-Based Spatial method proposed by Du *et al.* (2015) to construct the image and also, automatically, calculated the minimum ($V_{MIN}$) and maximum ($V_{MAX}$) velocities measured in the disks along the different measurement routes. Using the range between $V_{MIN}$ and $V_{MAX}$, velocity ranges associated with colors were manually adopted. To facilitate discussion in this paper, ten velocity bands associated with different percentages of the $V_{MAX}$ obtained in the disk were used. This procedure enabled the comparison of the images from different disks. The large number of bands was used to obtain more detailed results in regard to the interferences that affected the velocity. The pattern established for the association of velocity bands with image colors was as follows: $V_{MIN}$ to 10% of $V_{MAX}$: red; 10% to 20% of $V_{MAX}$: orange; 20% to 30% of $V_{MAX}$: yellow; 30% to 40% of $V_{MAX}$: light green; 40% to 50% of $V_{MAX}$: dark green; 50% to 60% of $V_{MAX}$: light blue; 60% to 70% of $V_{MAX}$: dark blue; 70% to 80% of $V_{MAX}$: pink; 80% to 90% of $V_{MAX}$: violet; and 90% to 100% of $V_{MAX}$: brown.

## RESULTS AND DISCUSSION

The inherent heterogeneity and orthotropy of wood led to velocity variations in the disks, even in those with a centered pith and no knots (Table 2). For all of the cases, the coefficient of variation (CV) of the velocities in the disks was higher than that of the disks from different logs.

**Table 2.** Average Velocities and CVs Along the Measurement Routes

| | Log Numbering - Disk | | | | | | | | |
|---|---|---|---|---|---|---|---|---|---|
| | 4-1 | 10-1 | 10-2 | 12-1 | 12-2 | 14-1 | 15-1 | 16-1 | 17-1 |
| Average Velocity* (m/s) | 1545 | 1783 | 1586 | 1684 | 1713 | 1675 | 1564 | 1659 | 1671 |
| CV | 13% | 12% | 12% | 12% | 12% | 11% | 10% | 10% | 11% |

*Average velocity of all of the logs considering the average speeds of the disks = 1653 m/s (CV = 5%)

Considering the results in Table 2, the tomographic image of a wooden disk was not expected to have a range of velocities (or colors), even under normal conditions (centered pith without deterioration or discontinuities), unless this range was quite broad. Wide ranges of velocity are not desirable in tomography because they limit the observation of deterioration. Figure 2 presents the tomographic image of one of the sample A disks, where the velocity was 60% to 90% of the $V_{MAX}$ (blue, pink, and violet).

The observed variability in the velocity in the ultrasonic tomography of the wood disks was also related to orthotropy (Dikrallah *et al*. 2006), unlike in the analyses of isotropic materials (Zeng *et al*. 2013). The velocities of the wave propagation in the radial direction were greater those in the tangential direction, which may affect the interpretation of the tomographic images (Socco *et al*. 2004; Li *et al*. 2014).

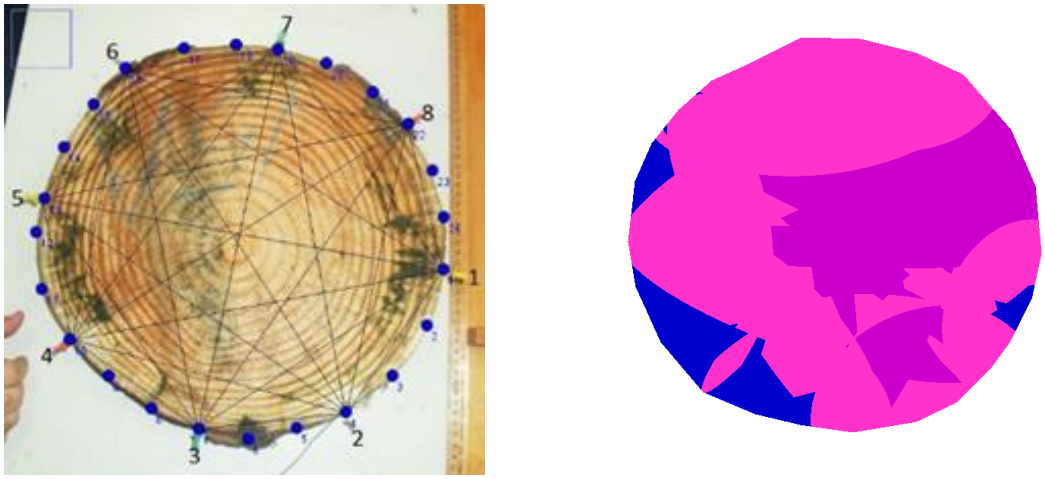


a b

**Fig. 2.** Example of a disk with a centered pith (a) and the image generated based on the ultrasound tomography results (b)
Legend: dark blue: 60% to 70% of $V_{MAX}$; pink: 70% to 80% of $V_{MAX}$; violet: 80% to 90% of $V_{MAX}$

Three significantly different groups existed in terms of the wave propagation velocity: radial direction (average $V_R$ = 1844 m/s), tangential direction considering the route through the disk ($V_{Ti}$ = 1706 m/s), and tangential direction at the edges ($V_{Tb}$ = 1151 m/s) (Fig. 3). Thus, the edge routes had the smallest velocities, as was also observed by Socco *et al*. (2004) and Du *et al*. (2015). This is highlighted in the tomographic image in Fig. 3. Du *et al*. (2015) concluded that the relation of $V_T/V_R$ varies with the angle between the tangential and radial directions and $V_T/V_R$ is minimized at angles ± 75°, which coincides with the external routes in the diffraction mesh.

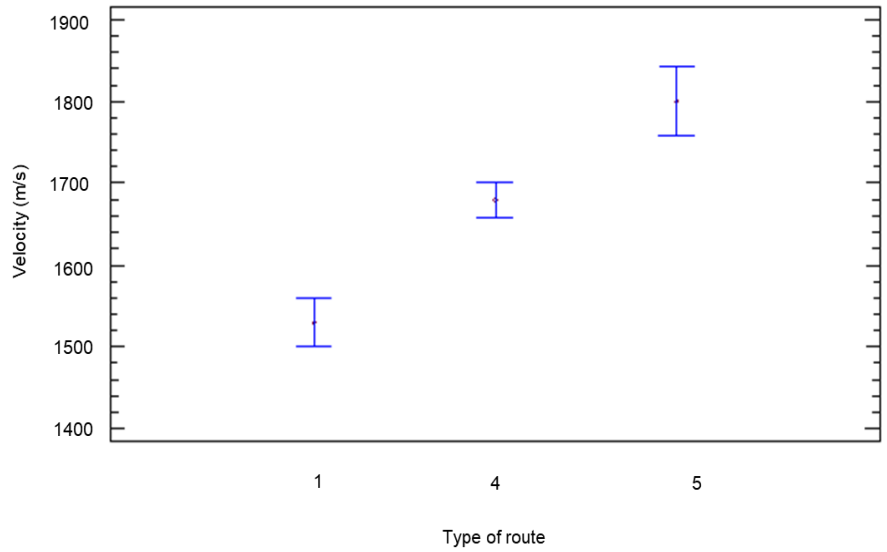


**Fig. 3.** Average wave propagation velocities (m/s) in the radial direction (5), internal tangential direction to the disk (4), and tangential direction at the edges (1) with the respective limits of the standard deviation (95% confidence)

For the routes passing through knots, increases in the radial and tangential velocities were observed (Fig. 5). The variability of the velocity also increased (Fig. 5) because this parameter depends on the size and number of knots through which the propagation waves travel. The same results were obtained by Riggio *et al*. (2015), who identified regions of higher velocity in ultrasound tomography images containing knots. In the multiple range test, five groups exhibited statistically different velocities, as shown in Fig. 4: tangential edge (1); tangential to the route through the disk, but not through a knot (4); radial velocity route not through a knot (5); tangential velocity through the disk and a knot (6); and radial velocity route through a knot (7).

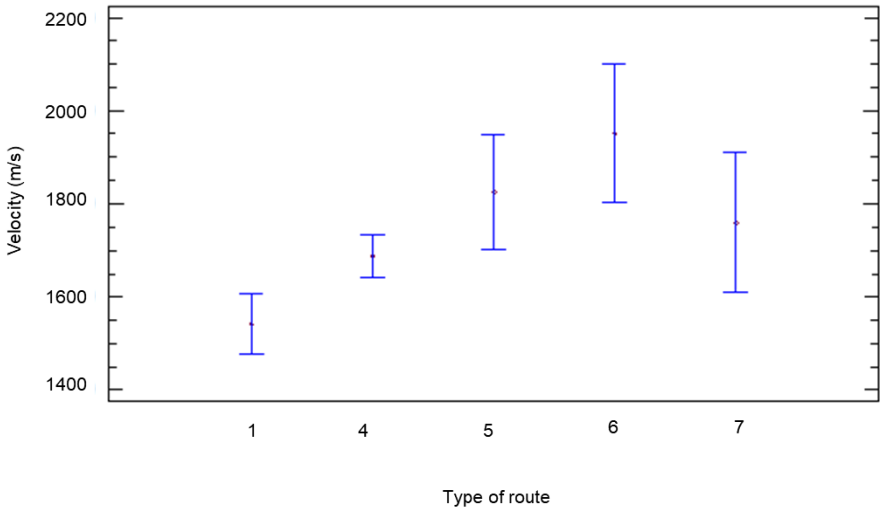


**Fig. 4.** Average velocities of the wave propagation (m/s) tangential to the edges (1), tangential through the disk, but not through a knot (4), tangential across the disk and passing through a knot (6), radial, but not passing through a knot (5), and radial through a knot (7) with their respective standard deviations (95% confidence)

The images of the disks with a centered pith and knots confirmed the results of the statistical analysis, which indicated that the velocity in the region of the knots was higher than that in the other regions of the disk, as shown in Fig. 5.

a b

**Fig. 5.** Example of a disk with a centered pith and knots (a) and the resulting image based on the tomographic ultrasound results (b)
Legend: light blue: 50% to 60% of $V_{MAX}$; dark blue: 60% to 70% of $V_{MAX}$; pink: 70% to 80% of $V_{MAX}$; violet: 80% to 90% of $V_{MAX}$; brown: 90% to 100% of $V_{MAX}$

In the case of the disks with a displaced pith and reaction wood, the multiple range test, applied to the velocities along the routes that actually passed through the zones of compression and opposition wood, revealed no statistical differences (Fig. 6). However, the average tangential velocities in the reaction (1593 m/s) and opposition (1541 m/s) wood zones were lower than the average velocities in the disks with a centered pith (1671 m/s). Additionally, the tangential edge velocities (1457 m/s) were statistically different from those of the reaction and opposition wood zones and lower than those along the routes through the disk (Fig. 6), as shown in the discussed cases.

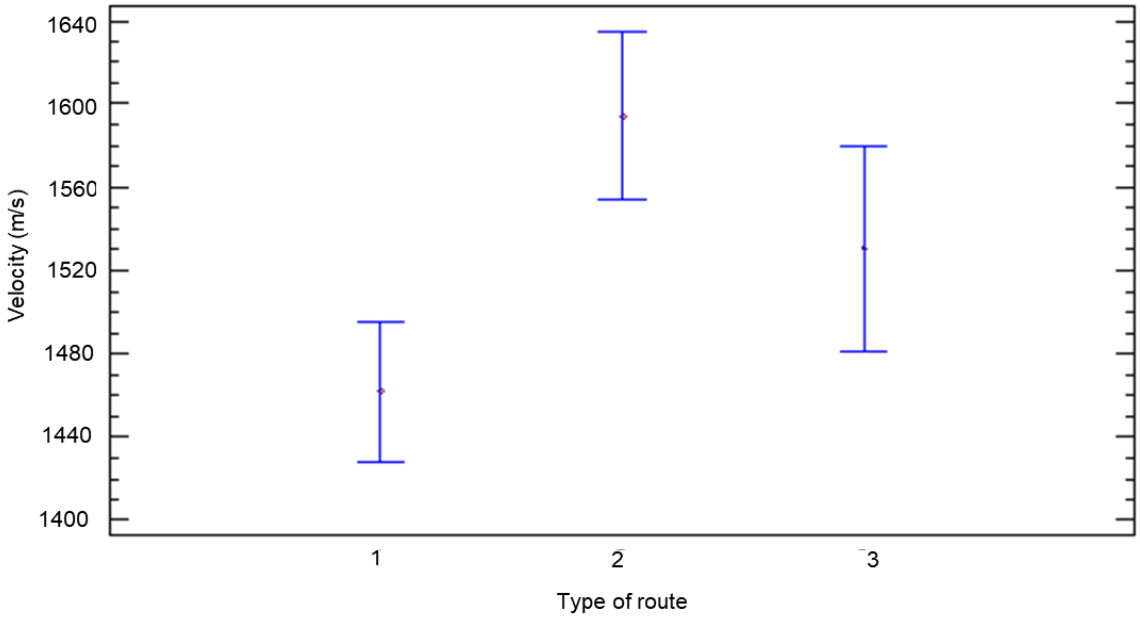


**Fig. 6.** Average values of the tangential velocities (m/s) at the tangential edge (1), tangential waves traversing the disk through compression wood (2), and tangential waves traversing the disk through opposition wood (3) with their respective standard deviations (95% confidence)

Although statistical differences in the velocity were not observed between the compression and opposition wood zones in the multiple range test (Fig. 6), the numerical values of the velocities in the compression wood were higher than those in the opposition wood. This finding was visualized in the ultrasonic tomographic images generated in the same disks (Fig. 7). This result may have been related to the higher percentage of lignin, higher density, higher proportion of latewood, and thicker walls of the tracheids in the compression wood (Ruelle 2014). Mohammad *et al*. (2011) measured lower ultrasound propagation velocities in the compression wood along the longitudinal direction, but higher velocity values along the transverse direction, as was observed in this study.

The comparison of average velocities using confidence interval (95% confidence) on disks with a displaced pith and only juvenile wood also revealed that the tangential velocities in the compression and opposition wood zones were statistically equivalent. However, the numerical values of the average tangential velocities were much lower (1385 m/s in the compression wood zone, 1395 m/s in the opposition wood zone, and 1260 m/s at the edges) than those in the mature wood. The tomographic images of these disks with juvenile wood showed a central zone with lower velocities (Fig. 8).

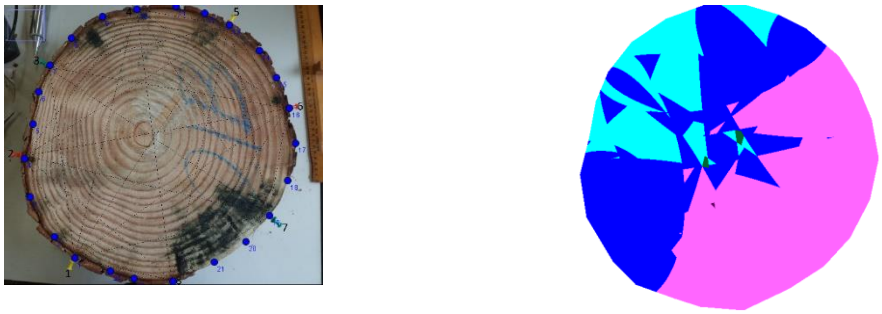

a b

**Fig. 7.** Example of a disk with a displaced pith (a) and the generated image based on the ultrasound tomography results (b)
Legend: light blue: 50% to 60% of $V_{MAX}$; dark blue: 60% to 70% of $V_{MAX}$; pink: 70% to 80% of $V_{MAX}$; violet: 80% to 90% of $V_{MAX}$; brown: 90% to 100% of $V_{MAX}$

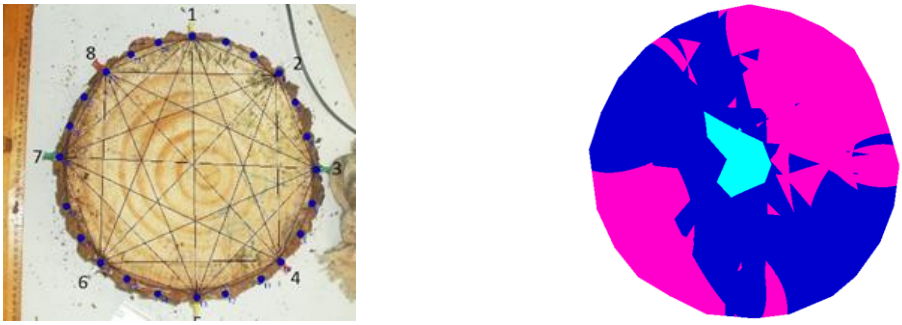

a b

**Fig. 8.** Example of a juvenile wood disk with a decentralized pith (a) and the generated image based on the ultrasonic tomography results (b)
Legend: light blue: 50% to 60% of $V_{MAX}$; dark blue: 60% to 70% of $V_{MAX}$; pink: 70% to 80% of $V_{MAX}$

The images of the disks obtained with ultrasonic tomography from samples A (centered pith and normal wood), B (centered pith and knots), and C (disk with mature wood and eccentric pith) showed that for *Pinus elliottii* disks, the velocities in the inner wood zone generally exceeded 70% of the $V_{MAX}$, whereas the velocities at the edges were approximately 60% to 70% of the $V_{MAX}$. Thus, variations in the propagation velocity of the ultrasonic waves caused by knots or reaction wood will not suggest the presence of a decay causing misinterpretation of the tomographical results.

In the case of the juvenile wood disks, although the velocity bands were always representative of the values obtained in the disks, the tomographical images showed that in the pith zone, the velocities were 50% to 60% of the $V_{MAX}$. Furthermore, the interior of the disks on tomography (Fig. 8) contained a significant blue area (60% to 70% of the $V_{MAX}$), whereas velocities in this range were only detected at the edges of the other disks (mature wood). Additionally, violet areas (80% to 90% of the $V_{MAX}$) disappeared. Brancheriau *et al*. (2012) also used ultrasound tomography to identify a region of lower velocity around the pith and determined that it corresponded to the presence of juvenile wood. The statistical analysis (average comparison and t-test) of the juvenile and mature wood disks revealed significant differences in the velocities (Table 3).

**Table 3.** Statistical Summary of the Velocities in the Tangential Direction in *Pinus elliottii* Disks Considering Propagation in Both Juvenile and Mature Wood

| | **Juvenile Wood** | **Mature Wood** |
|---|---|---|
| **Average Velocity (m/s)** | 1322 (a) | 1519 (b) |
| **Standard Deviation** | 248 | 284 |
| **CV** | 18.8% | 18.7% |
| **$V_{MIN}$ (m/s)** | 788 | 753 |
| **$V_{MAX}$ (m/s)** | 1950 | 2646 |
| t = 6.44 and P-value = 1.26 E-9: Rejection of the equality of averages hypothesis | | |

Different letters indicate significant differences. Statistical tests (average comparison and t-test) were applied with a 95% confidence level.

These results indicated that in wood containing a large proportion of juvenile wood, images may be misinterpreted because juvenile wood can be easily mistaken for decayed wood.

## CONCLUSIONS

1. The intrinsic variability of the wood was reflected in the wave propagation: radial velocities were greater than tangential ones, higher velocities in knot zones, and different velocities in reaction and opposition wood zones. Despite these variations, the velocities in the inner zones of the disks always exceeded 70% of the $V_{MAX}$ in the disk.

2. In the measurements using the diffraction mesh, the edge velocities, which were obtained in the tangential direction with the maximum angle from the radial direction, were always lower (60% to 70% of the $V_{MAX}$). Knowledge of these variations can improve ultrasound-based diagnosis and help avoid confusing natural reductions in velocity with those resulting from decayed zones.
3. More significant variations in the velocity were obtained in juvenile wood, where the velocities were 50% to 60% of the $V_{MAX}$ in the disk. Thus, the presence of a significant volume of juvenile wood in a trunk may be confused with the presence of deteriorated areas.

## ACKNOWLEDGMENTS

The authors would like to thank the Coordination of Improvement of Higher Level Personnel (CAPES) (Brasília, Brazil) for the scholarships and the Sao Paulo Research Foundation (FAPESP) (São Paulo, Brazil) (Proc. 2015/05692-3) for the research funding.

## REFERENCES CITED

Beall, F. C. (2002). "Overview of the use of ultrasonic technologies in research on wood properties," *Wood Sci. Technol.* 36(3), 197–212. DOI: 10.1007/s00226-002-0138-4

Brancheriau, L., Ghodrati, A., Gallet, P., Thaunay, P., and Lasaygues, P. (2012). "Application of ultrasonic tomography to characterize the mechanical state of standing trees (*Picea abies*)," *J. Phys. Conf. Ser.* 353(1), 1-13. DOI: 10.1088/1742-6596/353/1/012007

Bucur, V. (2003a). "Techniques for high resolution imaging of wood structure: A review," *Meas. Sci. Technol.* 14(12), 91-98. DOI: 10.1088/0957-0233/14/12/R01

Bucur, V. (2003b). *Nondestructive Characterization and Imaging of Wood*, Springer-Verlag, Berlin, Germany.

Bucur, V. (2006). *Acoustics of Wood*, Springer-Verlag, Berlin, Germany.

Bucur, V., and Chivers, R. C. (1991). "Acoustic properties and anisotropy of some Australian wood species," *ACTA Acust.* 75(1), 69-75.

Dikrallah, A., Hakam, A., Kabouchi, B., Brancheriau, L., Baillères, H., Famiri, A., and Ziani, M. (2006). "Experimental analysis of acoustic anisotropy of green wood by using guided waves," in: *ESWM-COST Action E35*, Florence, Italy, pp. 149-154.

Du, X., Li, S., Li, G., Feng, H., and Chen, S. (2015). "Stress wave tomography of wood internal defects using ellipse-based spatial interpolation and velocity compensation," *BioResources* 10(3), 3948-3962. DOI: 10.15376/biores.10.3.3948-3962

Guindos, P., and Guaita, M. (2013). "A three-dimensional wood material model to simulate the behavior of wood with any type of knot at the macro-scale," *Wood Sci. Technol.* 47(3), 585–599. DOI: 10.1007/s00226-012-0517-4

Guindos, P., and Polocoser, T. (2015). "Numerical calculations of the influence of the slope of grain on the effect of knots," *Eur. J. Wood Wood Prod.* 73(2), 271-273. DOI: 10.1007/s00107-014-0876-7

Hamm, E. A., and Lam, F. (1989). "Compression wood detection using ultrasonics," *G Prove Nondestructive* 1, 40-47.

Haygreen, J. G., and Bowyer, J. L. (1995). *Forest Products and Wood Science: An Introduction*, Iowa State University Press, Ames, IA.

Katz, J. L., Spencer, P., Wang, Y., Misra, A., Marangos, O., and Friis, L. (2008). "On the anisotropic elastic properties of woods," *J. Mater. Sci.* 43(1), 139-145. DOI: 10.1007/s10853-007-2121-9

Kollmann, F. F. P., and Côte, W. A. (1984). *Principles of Wood Science and Technology*, Springer-Verlag, New York, pp. 528-529.

Li, G., Wang, X., Feng, H., Wiedenbeck, J., and Ross, R. (2014). "Analysis of wave velocity patterns in black cherry trees and its effect on internal decay detection," *Comput. Electron. Agr.* 104, 32-39. DOI: 10.1016/j.compag.2014.03.008

Pellerin, R. F., and Ross, R. J. (2002). *Nondestructive Evaluation of Wood* (FPL-GTR-238), U.S. Department of Agriculture Forest Products Laboratory, Madison, WI, USA.

Puccini, C. T. (2002). *Avaliação de Aspectos de Qualidade da Madeira Utilizando o Ultra-som* [*Wood Quality Evaluation Using Ultrasound*], Doctoral Thesis, Universidade Estadual de Campinas, Campinas, Brazil.

Riggio, M., Sandak, J., and Franke, S. (2015). "Application of imaging techniques for detection of defects, damage and decay in timber structures on-site," *Constr. Build. Mater.* 101, 1241-1252. DOI: 10.1016/j.conbuildmat.2015.06.065

Ruelle, J. (2014). "Morphology, anatomy and ultrastructure of reaction wood," in: *The Biology of Reaction Wood*, B. Gardiner, J. Barnett, P. Saranpää, and J. Gril (eds.), Springer-Verlag, Berlin, Germany, pp. 13-35.

Sani, L., Lisci, R., Moschi, M., Sarri, D., Rimediotti, M., Vieri, M., and Tofanelli S. (2012). "Preliminary experiments and verification of controlled pulling tests for tree stability assessments in Mediterranean urban areas," *Biosystems Engineering* 112(3), 218 – 226

Saadat-Nia, M., Brancheriau, L., Gallet, P., Enayati, A. A., Pourtahmasi, K., and Honarvar, F. (2011). "Ultrasonic wave parameter changes during propagation through poplar and spruce reaction wood," *BioResources* 6(2), 1172-1185. DOI: 10.15376/biores.6.2.1172-1185

Schubert, S., Gsell, D., Dual, J., Motavalli, M., and Niemz, P. (2009). "Acoustic wood tomography on trees and the challenge of wood heterogeneity," *Holzforschung* 63(1), 107-112. DOI: 10.1515/HF.2009.028

Socco, L. V., Sambuelli, L., Martinis, R., Comino, E., and Nicolotti, G. (2004). "Feasibility of ultrasonic tomography for nondestructive testing of decay on living trees," *Res. Nondestruct. Eval.* 15(1), 31-54. DOI: 10.1080/09349840490432678

Wang, X., Wiedenbeck, J., and Liang, S. (2009). "Acoustic tomography for decay detection in black cherry trees," *Wood and Fiber Science* 41(2), 127-137.

Zeng, L., Lin, J., Hua, J., and Shi, W. (2013). "Interference resisting design for guided wave tomography," *Smart Mater. Struct.* 22(5), 1-12. DOI: 10.1088/0964-1726/22/5/055017

Article submitted: August 21, 2017; Peer review completed: November 5, 2017; Revised version received and accepted; November 27, 2017; Published: February 26, 2018.
DOI: 10.15376/biores.13.2.2834-2845